Structural and Electrical Properties of Polymer Nanocomposite Films

Chandni Bhatt, Ram Swaroop and A.L. Sharma

Abstract A free standing transparent film of solid state polymer electrolyte based on PEMA/PVC+$NaPF_6$ with different compositions of nano sized TiO_2 in weight percent (x = 0, 1, 2, 7, 10, 15, 20) is synthesized by using standard solution cast technique. The homogeneous surface of above polymer composition is examined by FESEM. The microscopic interaction among polymer, salt and nano-ceramic filler has been analyzed by Fourier Transformed Infra-Red (FTIR) spectroscopy. The reduction of ion pair formation in polymeric separator is clearly observed on addition of nano-filler in the polymer salt complex film. Electrical conductivity has been recorded of the prepared polymeric separator which is of the order of $\sim 1.5 \times 10^{-5} Scm^{-1}$ after addition of nano-filler (15 % wt/wt) which support the FTIR results. Electrochemical potential window has been observed of the order of ~ 6 V by the cyclic voltammetry results. The observed data of the prepared separator are at par with the desirable value for device application.

1 Historical Background

In 1833 Michael Faraday performed an experiment on ionic conductivity of inorganic solids. He observed enhancement in the value of electrical conductivity of Ag_2S with increasing temperature. At that time it was difficult to analyze because it was on strong contradiction to the behavior of metallic phases. Faraday reported similar observations on several other inorganic solids, in 1838. In 1851, Hittorf

C. Bhatt · R. Swaroop · A.L. Sharma (✉)
Centre for Physical Sciences, Central University of Punjab, Mansa Road, Bathinda 151001, Punjab, India
e-mail: alsharmaiitkgp@gmail.com

C. Bhatt
e-mail: bhattchandni84@gmail.com

R. Swaroop
e-mail: ramcuhp11pas18@yahoo.com

V.K. Jain et al. (eds.), *Recent Trends in Materials and Devices*,
Springer Proceedings in Physics 178, DOI 10.1007/978-3-319-29096-6_50

investigated that electrolytic conduction mechanism had exist in material Ag_2S and Cu_2S from decomposition during current flow.

In 1884, Warburg verify Faraday's law during electrolysis between sodium amalgam electrodes by using soda lime glass or crystalline SiO_2, founded that sodium ions migrate through solids. The first major invention by Nernst of an electric lighting device by using solid electrolytes. Nernst lamp was replaced by tungsten filament lamp in 1905—this gave a path in the development of solid state Ionics.

Haber was the first to give patent on electrical energy production from coal and gaseous fuels using solid electrolyte cell. In 1908, Katayama reported various cells based on solid electrolytes. In 1920, Tubandt and Eggert confirmed the validity of Faraday's laws of electrolysis for the case of solid-ionic conductors. In 1935, Schottky file a patent on fuel cell using solid electrolytes, halides, sulfates, carbonates, and phosphates, but no oxides. In 1950, Wagner studied thermodynamic and kinetic properties of materials by using solid electrolyte cells. Also Wagner improved direct current polarization technique with blocking electrodes for the determination of partial ionic and electronic conductivities of mixed conductor, which was based on Hebb idea, now it is known as Hebb-Wagner polarization technique.

In 1960, solid electrolytes of light weight and high power density batteries with the fulfillment of sufficient ionic conductivity was developed, for e.g. $RbAg_4I_5$. In 1967, Yoo and Kumer developed sodium-sulfur battery by performing an experiment in which molten sodium and sulfur separated by a Na^+-ion conductive membrane of β-Al_2O_3. This research gave an impulse to the growth of solid state ionics because it was working as alternative for liquid electrolyte system.

In 1973, further enhancement in ionic conduction was done by Liang with the dispersion of small particles of Al_2O_3 in the matrix of moderate ionic conductor LiI. Founded material was heterogeneous, having conductivity 50 times higher ionic conductivity than homogeneous LiI. This doping effect was further confirmed by Wagner and Maier for numerous other ionic conductor and interpreted as space charge layer model, in 1984. This enhancement is expected due to the properties of nanostructured material, which is a very active topic of research in the field of solid state ionics [1].

2 Introduction

There are two types of conduction in materials that is electronic and ionic conduction, electronic conduction are those in which electrons/holes are charge carriers whereas in ionic conduction the charge carriers are ions. Firstly, the ionic conductivity on inorganic solids has been studied by Michael Faraday in 1833. There was large enhancement in electrical conductivity of Ag_2S with increasing temperature. But it was became difficult to observe behavior of metallic phases at that time. But in the year 1978, Professor M.B. Armand highlighted the significance of

polymer electrolyte as a medium of ion transport which is capable of dissolving salts in a meeting held at University of St Andrews. Polymer electrolytes is now topic of interest for researcher in the development of battery technology. Solid state polymer electrolyte with high ionic conductivity have been desired for all solid state battery due to the reason that solid electrode/solid electrolyte contact. Flexible material like organic polymers can produce excellent solid/solid interface between solid electrode and solid electrolyte.

As portable electronics is becoming more and more common in our society, and many aspects of our lives are now dependent on the performance of our portable electronics, demand for safe, reliable and efficient mean to store electrical energy for portable devices has increased. Also, recent advances in processing power, screen size and urge for thinner and lighter devices, have increased the demand for lighter batteries with higher energy density. Li ion batteries have high voltage and energy density so they have great demand in electronics market. The outstanding energy capacity, high volumetric density and long life cycle of Li ion batteries have made them preferred choice for application in portable electronics and electric vehicles. Widespread use of Li ion batteries growing demand for Li commodity chemically. These demand raised question whether the Li natural reserves will continue to meet industrial needs in a commercially viable manner [2].

But there are several drawbacks that mostly found in Li ion batteries like flammability, leakage of the toxic electrolyte, rapid degradation of cathode material and cost of procuring and using Li metal [3].

Sodium is light alkali metal with single electron in outermost shell. This metal exhibit unexpected complexity properties [4]. Sodium are more environmentally friendly than Li, less expensive, more abundant, easily distributed and easier to extract than lithium [5]. Although sodium has molecular weight 23 g mol^{-1}, which is three times heavy than Li. But because of sodium is fourth most abundant element in earth crust and easy to recycle, it is used for sodium ion batteries. Sodium batteries provide low cost energy storage device, they operate at ambient temperature [6].

Polymer electrolyte act as a electrolyte cum separator material in batteries, because by using polymer electrolyte one can obtain flexible, compact, solid state structure that is free from leaks, free standing consistency, high ionic conductivity. Their main purpose is to separate anode and cathode material in batteries and act as ions transport medium for the conduction of ions during the electrochemical process that is charging and discharging, the ions in the electrolyte adsorb and desorb on the porous electrode. Which cause rapid charging and discharging of the polymer so that the capacitor like performance is obtained [7]. In most system conductivity much lower than the desirable values for the device application under surrounding conditions. The factor responsible for that are—low ambient ionic conduction, concentration polarization, poor stability (thermal, mechanical and electrochemical) [8]. These factor are due to the fact that slow ion movement in host polymer because of poor chain mobility in polymer, also ion—ion interaction [9].

PEO based polymer electrolyte are mostly used but PEO has high degree of crystalline behavior, the ionic conductivity of PEO-based electrolytes is low and

varies from 10^{-8} to 10^{-4} Scm^{-1} at temperature between 40 and 100 °C. The use of poly (ethyl methacrylate) (PEMA) as a host polymer was first reported by Han et al. and Fhamy et al. PEMA shows excellent chemical and high surface resistance and offers high optical transparency. Poly (vinyl chloride) (PVC) can act as a mechanical stiffener in the electrolyte due to its immiscibility with the plasticizer.

Various approaches are carried out by scientist to improve the conductivity of polymer electrolyte. As the ion motion is faster within the amorphous region than crystalline, so therefore various method employed to increase the amorphous nature of polymer, reduce crystalline phase and hence increasing ionic conductivity. The addition of nano-sized inorganic ceramic fillers particles such as Al_2O_3, SiO_2, TiO_2, ZrO_2 etc. in host polymer and other the addition of low molecular weight plasticizers such as ethylene carbonate (EC), propylene carbonate (PC), dimethyl carbonate (DMC), polyethyleneglycol (PEG) [10].

In this work, investigation of solid state polymer electrolyte cum separator is fabricated by taking various composition of TiO_2 nano-filler added in PEMA/PVC polymer blend complexed with anatomic ratio of (O/Na = 20) $NaPF_6$ salt. Addition of nano-filler with different composition increases interaction between polymer and nano-filler.

2.1 Advantage of Solid Electrolyte

Initially liquid electrolyte was used for battery application, but these batteries suffer from several problems. So these batteries are replaced by solid electrolyte which contain following qualities.

- Absence of liquid containment.
- No leakage problems.
- Moldability and miniaturization shape.
- Ability to operate with more highly reactive electrodes over a wider range of temperature.
- Possess High ionic conductivity and negligible electronic conductivity.
- Suitable mechanical properties.
- Stability with respect to adjacent phases and to thermal and electrochemical decomposition.
- Easy to fabricate.
- Reasonable cost.

3 Experimental Work

3.1 Material and Material Method

Following polymer, salt and nano-filler is to be used for the synthesis of free standingpolymer electrolyte film are Poly (ethyl meth acrylate) (PEMA), and Poly (vinyl chloride) (PVC) purchased from Sigma Aldrich as shown in Table 1.

Preparation of solid state polymer electrolytes
The solution cast technique was used for preparation of free standing thin film of polymer electrolyte. In solution cast method appropriate amount of polymer is dissolved in solvent. The solvent should be water free and boiling point not exceed from 65 °C. At the same time appropriate amount of complexing salt is also dissolved in same solvent. Solvent should be a common for both salt and polymer [11].

Procedure In experiment the pure polymer blend of composition (PEMA/PVC) films complexed with $NaPF_6$ salt prepared by solution cast technique. The weight percent ratio such as 50 weight percent of PEMA, PVC, and salt of Ö/Na ratio is 20 mixed by a solution casting technique using THF (Tetrahydrofuran) as solvent. The solution of above composition mixed for several hours by means of stirrer, until the solution mixed properly, and then casted onto polypropylene dishes and left for evaporation at room temperature, dried under vacuum at 10^{-3} m bar pressure for 2–3 days. Whereas in another samples the same polymer blend nanocomposites doped with different composition of nano-filler (TiO_2) was prepared in different proportion such as 1, 2, 5, 7, 10, 15, and 20 weight percent. The above composition of TiO_2 is added as a dopant, and stirred for about 10 h. These solutions were cast and left for evaporation with a similar manner. Finally the free standing film of pure and doped polymer electrolyte is obtained. Fig. 1 shows the schematic flowchart of solution cast technique.

Table 1 Shows material selection for polymer nanocomposite films based on $(PEMA/PVC)_8NaPF_6$ + x wt% TiO_2 nano-filler

Sr. no.	Name of material	Glass transition temperature (°C)	Melting point (°C)	Density (g/cm^3)
1	PEMA	66	120	1.119
2	PVC	80	240	1.385

Salt $NaPF_6$ (sodium hexafluorophosphate), m.pt. 200 °C, molar mass 167.95 g/mol, and density 2.369 g/cm^3
Nano-filler/Plasticizer TiO_2 nanoparticle

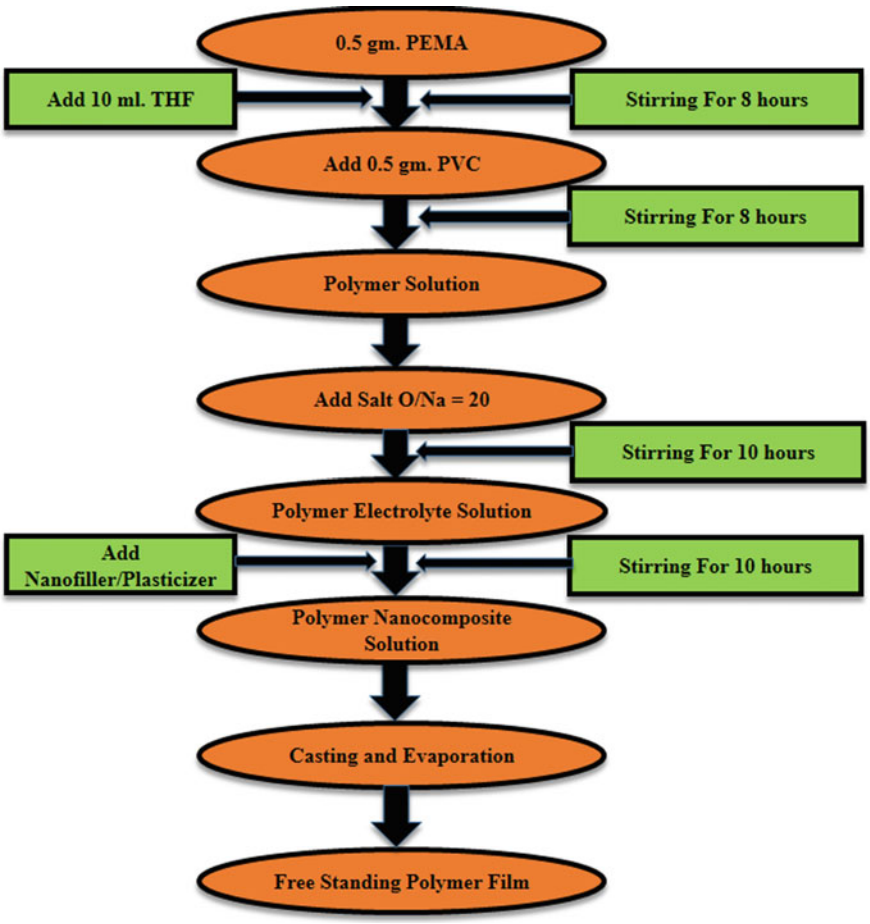

Fig. 1 Flow chart of solution cast technique

4 Experimental Techniques

FESEM To understand the properties of any material it is very necessary to understand the structural morphology of ions in the solid polymer electrolyte film, as the properties of material are closely related to its structure. Microstructural characterization of solid was done by field emission scanning electron microscopy [FESEM (Card Ziess Merlin Compact)] to investigate the influence of salt on polymer surface and morphology.

Impedance Spectroscopy Impedance spectroscopy was carried out for conductivity measurement with CHI electrochemical workstation over the frequency range

1 Hz to 1 MHz, the sample sandwiched between stainless steel electrodes and an a.c signal is applied.

FTIR Fourier Transform Infrared (FTIR) spectroscopy was done by Bruker Tensor-27, and spectrum was observed in the range of 600–4000 cm^{-1} to detect the presence of various functional groups. In infrared spectroscopy, IR radiation is passed through a sample. Some of the infrared radiation is absorbed by the sample and some of it is passed through (transmitted). The resulting spectrum represents the molecular absorption and transmission, creating a molecular fingerprint of the sample.

Electrochemical Analysis For electrochemical devices such as batteries, capacitors and electrochromic devices the electrochemical stability window curve is very necessary, observed by cyclic Voltammetry (CV) technique in the voltage range between −3 V and +3 V at scan rate of 0.1 V/s.

5 Result and Discussion

5.1 SEM Analysis

The properties associated with polymer nanocomposites are a function of the filler size, shape, dispersion, and of the polymer matrix - filler interaction. The morphological and structural analysis of nanocomposites is often done with scanning electron microscopy (SEM). Phase separation in polymer electrolyte due to rapid evaporation of solvent are shown by various pores in micrograph image Fig. 2a. The difference in pores is due to the difference in driving force for phase separation. The polymer with the nano-filler (TiO_2) lessen the difference in driving force for phase separation and produce homogeneous film of better quality.

Agglomerations in Fig. 2 (b) results due to weaker polymer/nano-filler interfacial interactions and higher stress concentration regions. As the dispersed particle size becomes smaller and the particle dispersion is more uniform then homogeneous film was produced which have better electrical as well as mechanical properties [12].

5.2 Electrical Conductivity

The electrical conductivity of polymer blend nanocomposite has been evaluated by using complex impedance spectroscopy technique. The representative complex impedance spectrum pattern of polymer nanocomposite film at x wt% (0, 7, 15, and 20) concentration of TiO_2 at room temperature is shown in Fig. 3. As shown in Fig. 3 the semicircular arc in the lower frequency region followed by rising spike in

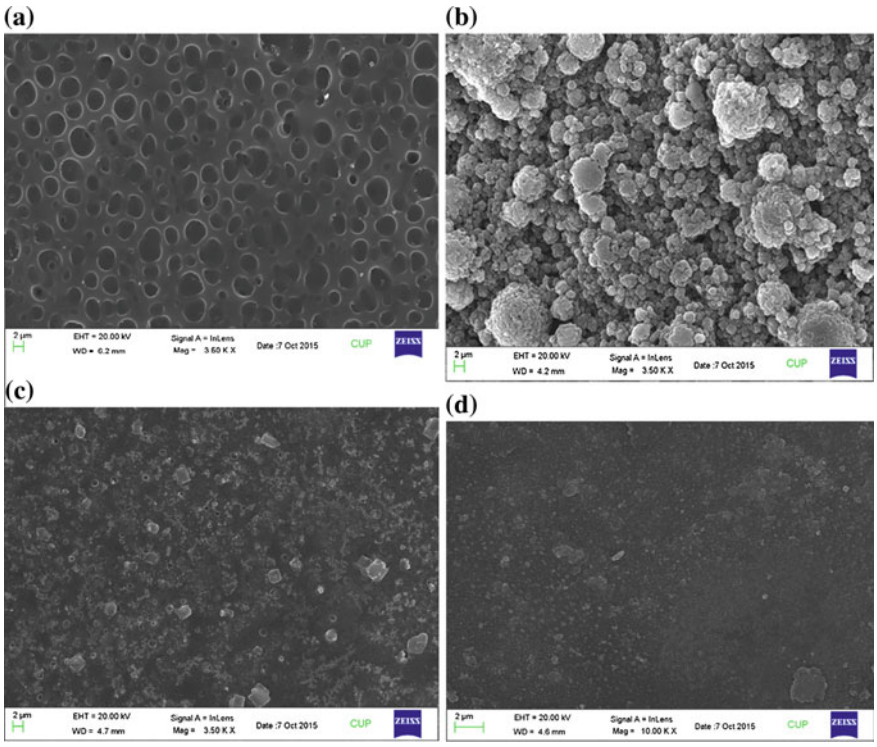

Fig. 2 FESEM micrograph of polymer electrolyte for **a** PEMA/PVC + $NaPF_6$ **b** PEMA/PVC + $NaPF_6$ + 7 wt% TiO_2 **c** PEMA/PVC + $NaPF_6$ + 15 wt% TiO_2 **d** PEMA/PVC + $NaPF_6$ + 20 wt% TiO_2

the higher frequency region on the real axis shows estimated values for bulk resistance (R_b). Conductivity will be measured with the help of following formula.

$$\sigma = t/R_b A$$

where't' is thickness of the polymer electrolyte in cm, which can be measured with the help of Barmier calliper, 'A' is the area of blocking electrode in cm^2, and R_b is the bulk resistance. The bulk resistance will be measured from the frequency intercept on the real axes [13]. With the addition of nano-filler and plasticizer, there is enhancement in conductivity was absorbed as shown in Table 1. Initial conductivity without addition of nano-filler, it is in the range of 10^{-9} S/cm, but with the addition of nano-filler it becomes 1.5×10^{-5} S/cm because addition of nano-filler improves the host polymer amorphous region by slowing the recrystallization rate.

A nonlinear least square fitting of impedance response of all samples agrees well with electrical equivalent circuit model comprising a series combination of constant phase element (CPE) with another constant phase element (CPE) and resistance

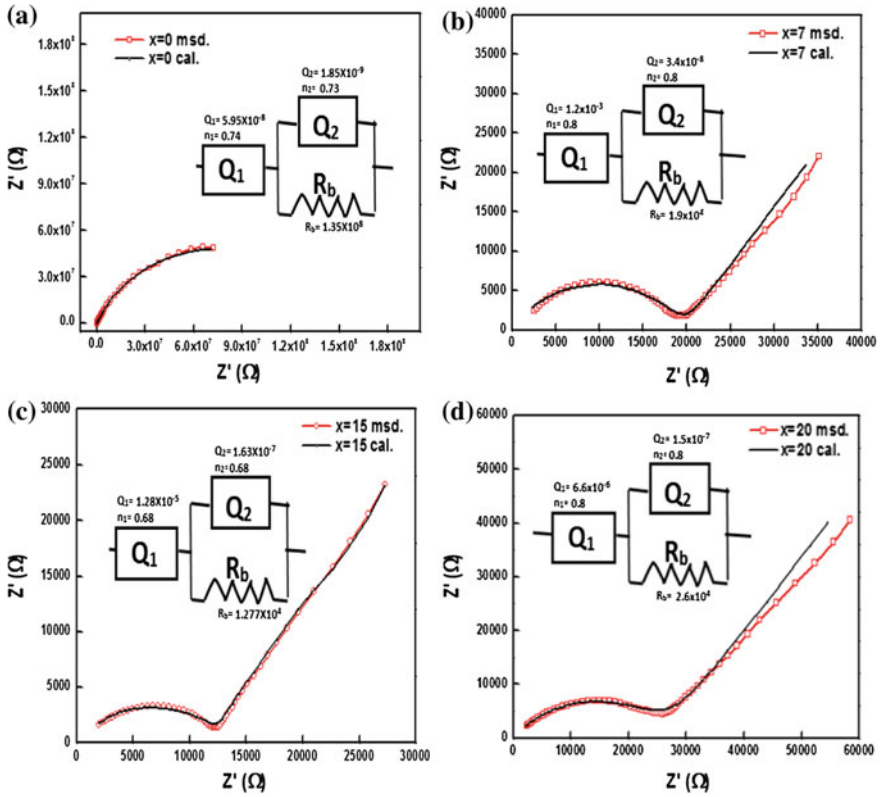

Fig. 3 Electrical impedance spectroscopic measurement of polymer nanocomposite (PEMA/PVC + $NaPF_6)_8$ + x wt% TiO_2 (x = 0, 7, 15, 20)

(R_b) also shown in Fig. 3. CPE describe both crystalline and amorphous phase of polymer nanocomposite film [14]. The conductivities values obtained for x = 0, 15 wt% concentration TiO_2 are 1.5×10^{-9}, 1.5×10^{-5} Scm^{-1}. The impedance of CPE is normally represented as.

$$Z_{CPE} = \frac{1}{Q_0(i\omega)^n}$$

where $i = (-1)^{1/2}$, "Q_0" and "n" are fitting parameter, it may behave as an electrical analogue of resistance, Warburg impedance capacitance and inductance for different values of 'n' [8].

In Table 2 there is continous increase in conductivity with the addtion of nano—filler up to x = 15 wt% concentration of TiO_2. But there is further decrease in the value of ionic conductivity for further addition of nano-filler. This is may be due to gradual formation of neutral aggregates of nano-filler, which creates blockages in the conducting path, reduces free volume, and increase crystallinity of the polymer

Table 2 Shows ionic conductivity of polymer nanocomposite films based on $(PEMA/PVC)_8NaPF_6$ + x wt% TiO_2 nano-filler

Polymer electrolyte	Nano-filler TiO_2 (in wt%)	Bulk resistance (R_b) In (Ω)	Conductivity (S/cm)
(PEMA/PVC + $NaPF_6$)	0	1.3×10^8	1.5×10^{-9}
(PEMA/PVC + $NaPF_6$)	7	1.9×10^4	1.0×10^{-5}
(PEMA/PVC + $NaPF_6$)	15	1.2×10^4	1.5×10^{-5}
(PEMA/PVC + $NaPF_6$)	20	2.6×10^4	7.8×10^{-6}

blend film. These factor may be responsible to resist the movement of mobile ions and polymer segments through the polymer matrix. Moreover, the formation of neutral aggregates also lower the number of mobile ions participating in conduction process. All these factors reduce the ion and segmental mobility through the polymer blend and hence, lead to the drop in conductivity [15]. We observe this type behavior of prepared polymer nanocomposite film at x = 20 wt% concentration of doped TiO_2.

5.3 FTIR

Fourier Transfer infrared (FTIR) microscopy analysis of the sample was done to detect the presence of various functional groups. FTIR spectrum was observed in the range of 600–4000 cm^{-1} as shown in Fig. 4. Also shift in peak position with addition of salt was clearly seen in Fig. 4. Because Na^+ ion from $NaPF_6$ was attracted toward the negative charge lone pair on oxygen atoms of carbonyl (C=O) and (C–O–C_2H_5) groups in PEMA. Carbonyl stretching [ν (C=O)] and asymmetrical O–C_2H_5 [ν (O–C_2H_5)] bending of PEMA was upshifted toward higher wavenumber. Which confirms the coordination of Na^+ ions of $NaPF_6$ on the oxygen atom of carbonyl group of PEMA. The peak in the wavenumber range 800–900 cm^{-1} corresponds to salt which causes due to the vibrational mode of PF_6^- anion. The characteristic absorption peak observed in the spectral pattern at the wavenumbers ~749, ~1149-52-53-54, ~1163-75-76-75-62, ~1388-89 and 2988 cm^{-1} are attributed to rock(CH_2), ν_a(C–O–C), υ(CO), τ(CH_2) and ν(C–H) mode of PEMA respectively [16]. The FTIR peaks at ~967-68-65, ~1064-65, ~1247-48-50-51 cm^{-1} are related to rock(C–H_2), stretching of C–C, def(C–H) of CHCl in PVC. The vibrational peak at 2988 $cm^{-1}$are assigned to asymmetric stretching of CH_2 [17]. One additional peak at ~1633-34-35-36 cm^{-1} due to the H–O–H group from TiO_2.

Characteristic absorption peak observed in the spectral pattern in the wavenumber 600–4000 cm^{-1} was shown with the help of band assignment in Table 3. Peak due to the vibrational modes of PF^{6-} anion has been observed at 847 cm^{-1}. Asymmetric stretching observed on peak keeps on changing with change in the nanofiller concentration in the composite phase [18].

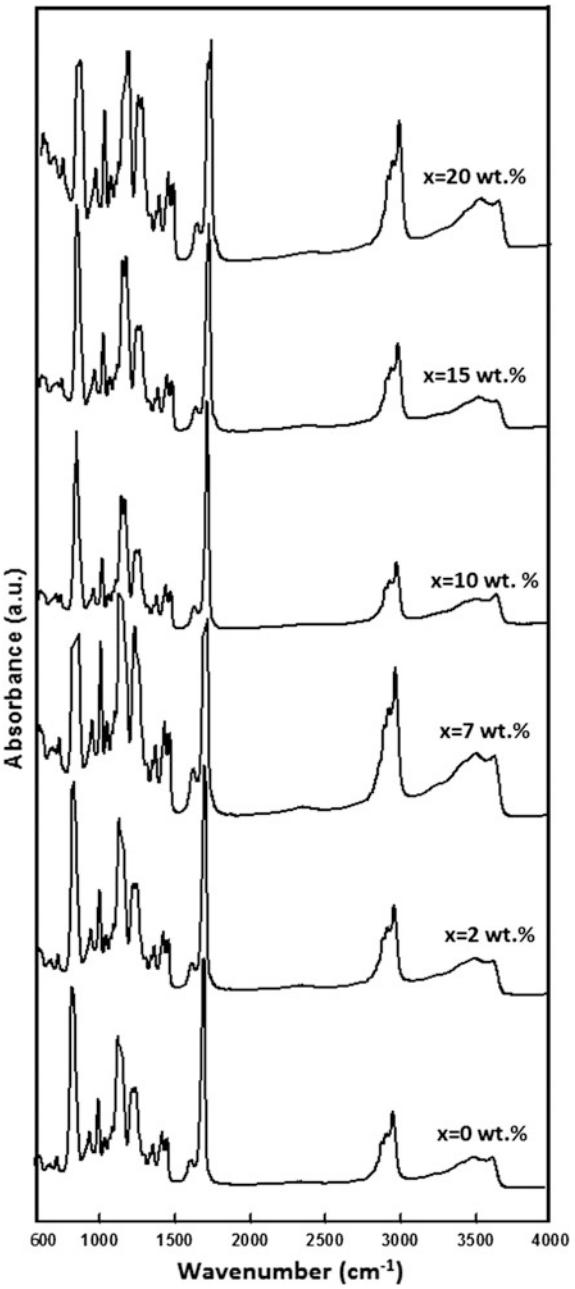

Fig. 4 FTIR spectra for polymer nanocomposite (PEMA/PVC + $NaPF_6)_8$ + x wt% TiO_2 (x = 0, 1, 7, 10, 15, 20) in in wavenumber 600–4000 cm^{-1}

Table 3 FTIR band assignment of polymer nanocomposite films based on $(PEMA/PVC)_8NaPF_6$ + x wt% TiO_2 nano-filler

$(PEMA/PVC)_8NaPF_6$ x = 0	$(PEMA/PVC)_8NaPF_6$ + x wt % TiO_2					Assignment mode	Source
	x = 2	x = 7	x = 10	x = 15	x = 20		
749	750	749	749	749	749	rock (C–H_2)	PEMA
845	847	853	853	846	849	ν (F_2P)	Salt
967	967	968	965	968	968	rock (C–H_2)	PVC
1064	1064	1065	1064	1065	1065	ν (C–C)	PVC
1154	1153	1149	1152	1152	1152	ν_a (C–O–C)	PEMA
1173	1173	1178	1176	1175	1162	ν (CO)	PEMA
1251	1250	1248	1247	1249	1249	def (C–H)	PVC
1389	1388	1388	1387	1388	1388	τ (C–H_2)	PEMA
1445	1446	1448	1448	1449	1447	ν (O–C_2H_5)	PEMA
1479	1479	1479	1480	1480	1481	δ (C–H_2)	PEMA
1633	1634	1634	1635	1635	1636	ν (H–O–H)	TiO_2
1720	1722	1729	1720	1725	1730	ν (C=O)	PEMA
2988	2981	2983	2982	2982	2981	ν (C–H)	PEMA

This asymmetry in the anion stretching vibrational mode is an outcome of the degeneracy arising out of more than one contribution possibly due to the presence of free anion and ion pairs.

In order to be sure the band pattern in the wavenumber 800–900 cm^{-1} has been deconvoluted using Voigt profile with a commercial software peak fit analyser. Two distinct contribution observed at 850 and 872 cm^{-1} in the deconvoluted pattern as shown in Fig. 5. The peak appearing at 850 cm^{-1} has been attributed to free anions and peak appearing at 872 cm^{-1} has been attributed to presence of ion pairs in the solid polymer electrolyte film [8].

Free anion area increases whereas ion pair area decreases with the addition of nano-filler up to certain limit of nano-filler that is x = 15 wt% TiO_2 here, further addition of nano-filler at x = 20 wt% TiO_2 nano-filler it decreases. Also Table 4 shows Peak position of deconvoluted free anion peak of polymer nanocomposite films based on $(PEMA/PVC)_8NaPF_6$ + x wt% TiO_2 nano-filler. The presence of two distinct degenerate FTIR band in the deconvoluted pattern for experimental spectrum provides an evidences of strong ion–ion interaction in the prepared polymer nanocomposite films.

5.4 Electrochemical Stability

For electrochemical devices such as batteries, capacitors and electrochromic devices, electrochemical stability window curve is very necessary. This stability window curve (Charging and discharging) for polymer blend electrolyte based on sodium ion batteries were observed by cyclic Voltammeter (CV) analysis. This

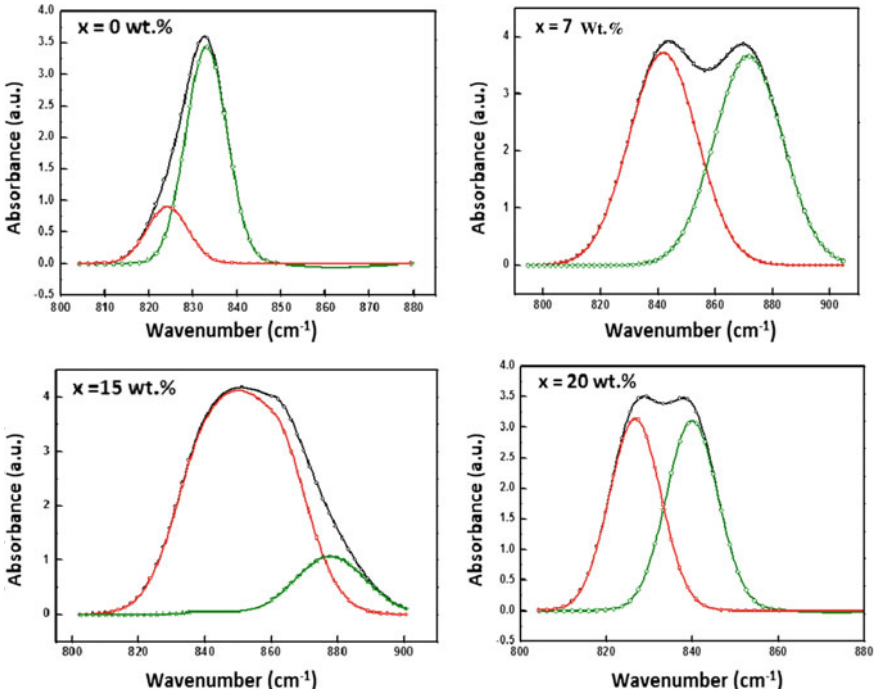

Fig. 5 Deconvolution pattern of ν (PF_6^-) in $(PEMA/PVC)_8NaPF_6$ + x wt% TiO_2 nano-filler

Table 4 Peak position of deconvoluted free anion peak of polymer nanocomposite films based on $(PEMA/PVC)_8NaPF_6$ + x wt% TiO_2 nano-filler

Nano-filler TiO_2 (in wt. %)	Deconvoluted anion peak data				Correlation coefficient (r^2)
	Free anion peak		Ion pair peak		
	Position (cm^{-1})	Area (%)	Position (cm^{-1})	Area (%)	
0	836	20.8187	850	79.1812	0.998
7	841	50.3925	871	49.6074	0.983
15	850	78.1155	872	21.8844	0.995
20	840	50.2524	862	49.7475	0.995

process was observed in the potential range of −3 to 3 V for x = 20 wt% as shown in Fig. 6. through blocking electrode of stainless steel. Electrochemical stability window curve is obtained in the range from about −3 to 3 V, which is an acceptable voltage range for device application [19, 20].

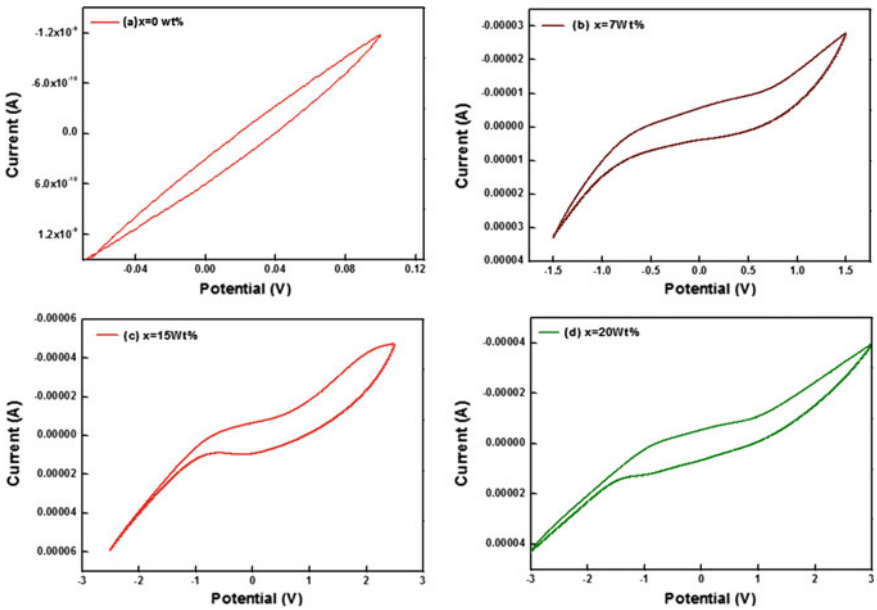

Fig. 6 Cyclic Voltammetry images of $(PEMA/PVC)_8NaPF_6$ + x wt% TiO_2 nano-filler

6 Conclusions

At $x = 0$ wt% of TiO_2 in polymer nanocomposite film was observed. The polymer with the nano-filler (TiO_2) lessen the difference in driving force for phase separation and produce homogeneous film at $x = 15$ wt% of nano-filler, and produce polymer film of better quality which can enhance the electrical as well as mechanical properties of prepared polymer films.

There is enhancement in conductivity. Without addition of nano-filler conductivity is in the range of 10^{-9} S/cm, but with the addition of micro range inorganic nano-filler it becomes 1.5×10^{-5}. Addition of nano-filler improves the host polymer amorphous region by slowing the recrystallization rate. A nonlinear least square fitting of impedance response of all samples agrees well.

FTIR confirms ion-polymer, polymer-polymer interaction and the presence of various functional groups present in prepared polymer electrolyte film by observing the spectra in the wavenumber 600–4000 cm^{-1}. The presence of two distinct degenerate FTIR band in the experimental spectrum provides an evidences of strong ion–ion interaction in the prepared polymer nanocomposite films.

Electrochemical stability window curve is obtained in the range from about −3 to 3 V for $x = 15$ and 20 wt%, which is an acceptable voltage range for device application.

Acknowledgments One of authors is thankful to Central University of Punjab for providing fellowship during M. Phil. Course and partial support received from the UGC Start-up-Grant (GP-41).

References

1. P. Knauth, H.L. Tuller, J. Am. Ceram. Soc. **85**(7), 1654 (2002)
2. F. Yuan, H.-Z. Cheng, H.-Y. Yang, H.-Y. Li, M. Wang, Mater. Chem. Phys. **89**, 390 (2005)
3. M. Mortazavi, J. Deng, B. Shenoy Vivek, V. Medhekar Nikhil, J. Power Sources **225**, 207 (2012)
4. K. Kiran Kumar, M. Ravi, Y. Pavani, S. Bhavani, A.K. Sharma, V.V.R. Narasimha Rao, J. Membr. Sci. **454**, 200 (2014)
5. Ho KhacHieu, Vacuum **120**, 13 (2015)
6. J. Serra Moreno, M. Armand, M.B. Berman, S.G. Greenbaum, B. Scrosati, S. Panero, J. Power Sources **248**, 695 (2014)
7. M.L. Verma, M. Minakshi, N.K. Singh, I & EC Res. **53**, 14993–15001 (2014)
8. A.L. Sharma, K. Awalendra Thakur, J. Mater. Sci. **46**, 1916 (2011)
9. H.P.S. Missan, B.S. Lalia, K. Karan, A. Maxwell, Mater. Sci. Eng. B **175**, 143 (2010)
10. H.M.J.C. Pitawala, M.A.K.L. Dissanayake, V.A. Seneviratne, Soild State Ionics **178**, 885 (2007)
11. A. Arya, A.L. Sharma, Appl. Sci. Lett. **2**(2), 72–75 (2016)
12. S. Rajendran, M. Ramesh Prabhu, M. Usha Rani, Int. J. Electrochem. Sci. **3**, 282 (2008)
13. Y.L. Ni'mah, M.-Y. Cheng, J.H. Cheng, J. Rick, B.-J. Hwang, J. Power Sources **278**, 375 (2014)
14. A.L. Sharma, A.K. Thakur, Ionics **19**(5), 795–809 (2013)
15. P. Joge, D.K. Kanchan, P. Sharma, N. Gondaliya, IOSR J. Appl. Phys. **1**, 55 (2014)
16. S. Rajendran, M.R. Prabhu, M.U. Rani, Int. J. Electrochem. Sci. **3**, 282 (2008)
17. N.F. Zain, N. Zainal, N.S. Mohamed, Phys. Scripta **90**, 015702 (2015)
18. P. Pradeepa, S. Edwinraj, M.R. Prabhu, Chin. Chem. Lett. **26**, 1191 (2015)
19. C. Cao, H. Wang, W. liu, X. Liao, L. Li, Int. J. Hydrogen Energy **39**, 16110 (2014)
20. A. Arya, S. Sharma, A.L. Sharma, M. Sadiq, J. Integr. Sci. Technol. **4**(1), 17–20 (2016)